Transition Analysis for the CRM-NLF Wind Tunnel Configuration

Pedro Paredes,* Balaji Venkatachari,†
National Institute of Aerospace, Hampton, VA 23666, USA

Meelan M. Choudhari,‡ Fei Li,§ Nathaniel Hildebrand,¶ Chau-Lyan Chang‖
NASA Langley Research Center, Hampton, VA 23681, USA

This paper reports the results of a comprehensive linear stability analysis of the boundary layer flow over the common research model with natural laminar flow (CRM-NLF) aircraft configuration. The flow conditions match selected test conditions from a recent wind tunnel experiment in the National Transonic Facility at the NASA Langley Research Center. Previous work has shown that the measured onset of laminar-turbulent transition during the experiments can be correlated with the linear amplification of Tollmien-Schlichting (TS) and stationary crossflow (CF) instabilities in the swept wing boundary layer. However, a significant scatter ($N \in (4, 9)$) was observed in the values of the logarithmic amplification factor along the measured transition front. This previous analysis was based on an approximate basic state (based on a boundary layer code with conical flow approximation) and parallel stability computations without surface curvature effects. Here, we examine the effects of these various approximations with the goal of quantifying the resulting changes in the N-factor correlations. Specifically, both linear stability theory (LST) and the parabolized stability equations (PSE) are used in conjunction with an accurate definition of the laminar boundary layer flow as computed with a Navier-Stokes solver with a Reynolds-Averaged-Navier-Stokes (RANS) based turbulence model within the turbulent parts of the flow. Furthermore, the effects of instability wave propagation within a fully three-dimensional boundary layer are also evaluated by integrating the disturbance growth rates along suitably chosen, curvilinear (i.e., nonplanar) propagation trajectories. The results of this analysis are also used in an accompanying paper by Venkatachari et al. to develop improved, physics based transition predictions for the same CRM-NLF configuration.

Nomenclature

AoA	=	angle of attack [deg]
C_f	=	skin friction coefficient
C_p	=	surface pressure coefficient
f	=	disturbance frequency [Hz]
η_w	=	semispan location nondimensionalized by semispan length
h_ξ	=	streamwise metric factor
h_ζ	=	spanwise metric factor
L	=	reference length [m]
m	=	azimuthal wavenumber
M	=	Mach number
N	=	logarithmic amplification factor
$\bar{\mathbf{q}}$	=	vector of base flow variables

*Research Engineer, Computational AeroSciences Branch, NASA LaRC. AIAA Senior Member
†Research Engineer, Computational AeroSciences Branch, NASA LaRC. AIAA Senior Member
‡Research Scientist, Computational AeroSciences Branch. AIAA Fellow
§Research Scientist, Computational AeroSciences Branch.
¶Research Scientist, Computational AeroSciences Branch. AIAA Member
‖Research Scientist, Computational AeroSciences Branch. AIAA Associate Fellow

$\tilde{\mathbf{q}}$	=	vector of perturbation variables
$\hat{\mathbf{q}}$	=	vector of amplitude variables
Re_{MAC}	=	Reynolds number based on mean aerodynamic chord
Re_∞	=	freestream unit Reynolds number [m^{-1}]
T	=	temperature [K]
(u, v, w)	=	streamwise, wall-normal, and spanwise velocity components [m s^{-1}]
(x, y, z)	=	Cartesian coordinates [m]
x/c	=	chordwise coordinate scaled by reference chord length
y^+	=	near wall grid spacing in wall units
α	=	streamwise wavenumber [m^{-1}]
β	=	spanwise wavenumber [m]
λ	=	spanwise wavelength [m^{-1}]
δ	=	boundary layer thickness [m]
κ_ξ	=	streamwise curvature [m^{-1}]
κ_ζ	=	spanwise curvature [m^{-1}]
ω	=	disturbance angular frequency [rad s^{-1}]
ρ	=	density [kg m^{-3}]
(ξ, η, ζ)	=	streamwise, wall-normal, and spansiwe coordinates [m]
Subscript		
∞	=	freestream value
tr	=	transition location
Superscript		
H	=	conjugate transpose

I. Introduction

Substanttial reductions in the fuel burn of future aircraft have been targeted both in the U.S. [1] and Europe [2] in order to lower the cost of air travel and alleviate the impact of aviation on the environment. A significant fraction of the targeted reductions in aircraft fuel burn will come from the reductions in vehicle drag. For today's commercial transport aircraft, up to one half of the total drag corresponds to skin friction drag. Because laminar skin friction is much lower in comparison with the turbulent skin friction, flow control via delayed boundary-layer transition over major aerodynamic surfaces holds the potential to provide the desired reductions in the overall drag.

According to the CFD Vision 2030 [3], the most critical area in computational fluid dynamics (CFD) simulation capability that will remain a pacing item for the foreseeable future is the ability to adequately predict viscous flows with transition-to-turbulence and flow separation. A majority of CFD computations are carried out under the assumption that the flow is turbulent everywhere, allowing the use of the computationally efficient Reynolds-averaged Navier-Stokes (RANS) based turbulence models throughout the flowfield. However, for several applications ranging from wings with natural laminar flow (NLF) technology, high-lift configurations, rotorcraft flows, and unmanned aerial vehicles, the strong assumption involving a fully turbulent flow can lead to significant errors in the prediction of relevant performance metrics. Furthermore, most of the RANS models are incapable of modeling the process of transition from laminar to turbulent flow because of the complexity involved in the physics of the transition onset process, and the inherent averaging process in the RANS procedure makes it difficult to capture the development of the linear disturbances that initiate the laminar-turbulent transition process within the initially laminar boundary layer as well as the subsequent nonlinear growth of those disturbances and the eventual breakdown to turbulence.

Direct numerical simulations (DNS) and wall-resolved large-eddy simulations (WRLES) are the only approaches capable of simulating the complete set of physical processes that result in the onset of transition and the breakdown of laminar boundary layers into a turbulent flow. However, even with the current state-of-the-art high performance computing tools, these approaches are too expensive to permit the analysis of realistic configurations at high Reynolds numbers due to the extreme requirements on spatio-temporal resolutions. Moreover, DNS and WRLES require accurate specification of the initial and boundary conditions to account for a correct representation of the disturbance environment that excites the instabilities in the flow, and this information is often not fully available from most wind-tunnel and flight tests.

Semiempirical correlations based on the linear stability theory (LST), such as the e^N method introduced by Smith and Gamberoni [4] and Ingen [5], remains one of the most widely used approaches for the prediction of transition onset locations in aircraft design computations. The LST equations are derived from the linearized Navier-Stokes equations to track the evolution of small amplitude, fixed frequency disturbances under the parallel flow assumption. The e^N method does require the specification of a critical N-factor that must be obtained from correlations against experimentally measured transition locations. Transition analysis using the parabolized stability equations (PSE) [6] involves less restrictive assumptions and can also account for the effects of a weakly nonparallel basic state, both streamwise and transverse curvatures in the surface geometry, and nonlinear modal interactions of the laminar instabilities. Both LST and PSE can account for the amplification of the dominant primary instabilities encountered on aircraft wings, namely, the Tollmien-Schlichting waves and the stationary and traveling crossflow vortices. However, the application of these approaches toward a coupled computation of laminar, transitional, and fully turbulent parts of a flowfield entails an increased computational cost as well as complexity; it also suffers from a lack of robustness and often requires adequate understanding of transition physics and hydrodynamic stability theory that typical users of CFD codes may not know. To alleviate or circumvent these shortcomings, surrogate models are often used in lieu of the direct computation of stability characteristics based on the laminar flow information provided by the flow solver. There are a number of successful implementations of CFD codes that combine stability-based transition predictions with RANS-based turbulence modeling, for instance see Refs. [7–14]. However, a majority of these models suffer from the need to have sufficiently well resolved boundary layer profiles in the laminar base-flow computations, including the wall-normal derivatives of velocities and temperature, or at least, the need to compute integral boundary layer parameters that may be used as a proxy to the laminar profiles themselves. These restrictions are difficult to overcome in the modern CFD codes that rely upon massive parallelization and the use of unstructured grids [15].

Given that the vehicle performance is often characterized in terms of integral quantities such as load/moment coefficients or through pressure/skin-friction distribution, capturing the detailed physics of the transition to turbulence in itself is less important than the overall impact of boundary layer transition on the development of the boundary layer and its impact on the aforementioned quantities. Due to the previously mentioned reasons and reduced requirements in terms of computational cost, research efforts to develop models that represent the transition physics and can still be embedded into a RANS framework have gained substantial ground [16–25]. For reasons of computational cost, these models often require that only local information be used to model transition, instead of using detailed boundary layer profiles for stability analysis or even integral-boundary layer parameters that may be used in metamodels for the stability characteristics. The RANS-based transition models often rely on solving additional transport equations and using correlations that determine the onset of transition, allowing the codes to switch between operating in the laminar and turbulent modes. This approach clearly overcomes some of the abovementioned limitations of stability-based transition prediction, and hence, is well-suited for generalizing the established process for turbulent flow computations in a cost effective manner. However, by virtue of lacking an adequate representation of the complex transition process, such models are also less amenable to an extrapolation to new configurations, and in general, must be validated on a case by case basis. More details on the various approaches currently being used to predict/model transition can be found in Refs. [26, 27].

The present research seeks to blend the so-called physics-based approach for transition modeling with the RANS-based approaches, with the eventual goal of developing a reliable and cost efficient, yet robust and user-friendly approach for integrated modeling of laminar-turbulent transition. To help achieve that goal, this particular paper is focused on a detailed assessment of transition prediction via linear stability correlations based on varying levels of fidelity in modeling the amplification of unstable disturbances in the boundary layer flow over a swept, tapered wing. This assessment is facilitated by the transition data obtained on NASA's common research model with natural laminar flow (CRM-NLF) [28–30] that was tested in the National Transonic Facility.

On a typical transport aircraft wing with moderate sweep, transition occurs as a result of crossflow (CF) instability and/or Tollmien-Schlichting (TS) instability, provided that the attachment line remains laminar. The CRM-NLF wing has been designed to modify the surface pressure distribution in such a way that the overall amplification of both of these instabilities is substantially reduced in comparison with that over a conventional wing. CF instability growth is attenuated through a rapid acceleration near the leading edge (achieved via a sufficiently small leading edge radius), while the amplification of the TS waves is controlled by creating a slightly favorable pressure gradient aft of the crossflow dominated leading edge region. The CRM-NLF design also addresses attachment line contamination and the possibility of transition due to attachment line instabilities, thereby allowing the laminar flow to be maintained over substantial regions of the wing, and thus, helping to reduce the total aerodynamic drag.

A bulk of the existing studies involving the transport-equation-based transition models have been carried out for low Mach number ($M_\infty < 0.3$) configurations and/or for modest wing-chord Reynolds numbers and with pressure distributions that may not be optimal for wing designs for subsonic transport aircraft flying at Mach numbers between

0.75 to 0.90. Given the sensitivity of transition to wind tunnel disturbances and the cost of flight experiments, computational tools will need to play an important role in the assessment of laminar flow designs for flight applications, both as a means of risk reduction and to help optimize the wing design. The CRM-NLF configuration supports the simultaneous presence of multiple potential transition mechanisms at realistic flight transport conditions, which makes this configuration a unique opportunity to examine how the RANS-based transition models perform. In that regard, the present paper also aims to provide useful guidance to improve the physical basis of the existing transition models as described in the accompanying paper by Venkatachari et al. [31].

The paper is organized as follows. § II provides a summary of the hierarchy of linear stability formulations used in this paper. Preliminary computational results pertaining to the mean flow over the CRM-NLF configuration are presented in §III. Finally, a summary of the present work and some concluding remarks are presented in §IV.

II. Theory

In what follows, we study the boundary layers over the wing of the CRM-NLF at conditions selected to match NASA's recent experiments on the same [28–30]. For this problem, the computational coordinates are defined as an orthogonal body-fitted coordinate system, (ξ, η, ζ) denote the streamwise, wall-normal, and spanwise coordinates and (u, v, w) represent the corresponding velocity components. Density and temperature are denoted by ρ and T. The metric factors are defined as

$$h_\xi = 1 + \kappa_\xi \eta, \tag{1}$$
$$h_\zeta = 1 + \kappa_\zeta \eta, \tag{2}$$

where κ_ξ and κ_ζ denotes the streamwise and spanwise curvatures. The Cartesian coordinates are represented by (x, y, z). The vector of perturbation fluid variables is $\tilde{\mathbf{q}}(\xi, \eta, \zeta, t) = (\tilde{\rho}, \tilde{u}, \tilde{v}, \tilde{w}, \tilde{T})^T$, the vector of amplitude functions is $\hat{\mathbf{q}}(\eta) = (\hat{\rho}, \hat{u}, \hat{v}, \hat{w}, \hat{T})^T$, and the vector of basic state fluid variables is $\bar{\mathbf{q}}(\eta) = (\bar{\rho}, \bar{u}, \bar{v}, \bar{w}, \bar{T})^T$. The streamwise and spanwise wavenumbers are α and β, respectively, and ω is the angular frequency of the perturbation. The spanwise wavelength is defined as $\lambda = 2\pi/\beta$.

The instability characteristics of the boundary layer over the CRM-NLF wing is calculated with linear stability theory (LST) and parabolized stability equations (PSE). The onset of laminar-turbulent transition is estimated using the logarithmic amplification ratio, the so-called N-factor, relative to the lower bound location ξ_{lb} where the disturbance first becomes unstable,

$$N(\omega, \beta) = -\int_{\xi_{lb}}^{\xi} \sigma(\xi', \omega, \beta)\, \mathrm{d}\xi'. \tag{3}$$

Accordingly, we assume that transition onset is likely to occur when the N-factor envelope reaches a specified value.

A. Linear Stability Theory

The quasiparallel LST assumes the boundary layer profiles to be locally parallel by dropping the streamwise derivative terms and setting the wall-normal velocity equal to zero. In the LST context, the perturbations have the form

$$\tilde{\mathbf{q}}(\xi, \eta, \zeta, t) = \hat{\mathbf{q}}(\eta) \exp\left[\mathrm{i}\left(\alpha\xi + \beta\zeta - \omega t\right)\right]. \tag{4}$$

Substituting Eq. (4) into the linearized Navier-Stokes (LNS) equations, an ordinary-differential-equation (ODE) based generalized eigenvalue problem (GEVP) can be written in the following form by using the companion matrix method [32] to reduce the quadratic terms in α from the viscous terms,

$$\mathbf{A}\hat{\mathbf{q}}^+ = \alpha \mathbf{B}\hat{\mathbf{q}}^+, \tag{5}$$

where $\hat{\mathbf{q}}^+(\eta) = (\hat{\rho}, \hat{u}, \hat{v}, \hat{w}, \hat{T}, \alpha\hat{u}, \alpha\hat{v}, \alpha\hat{w}, \alpha\hat{T})^T$. The entries of operators $\mathbf{A}$ and $\mathbf{B}$ are found in Refs. [33, 34]. The GEVP is solved by the inverse Rayleigh iteration method [35]. The imaginary part of the sought eigenvalue α correspond to the growth rate of the disturbance with a selected combination of ω and β.

$$\sigma_{LST}(\xi, \omega, \beta) = -\Im(\alpha) \tag{6}$$

B. Parabolized Stability Equations

In the PSE context, the streamwise curvature and nonparallel effects are considered. The PSE approximation is based on isolating the rapid phase variations in the streamwise direction. The effects of instability wave propagation within a fully three-dimensional boundary layer can also be evaluated by performing the parabolic integration along stream or group velocity lines. The perturbations have the form

$$\tilde{\mathbf{q}}(\xi,\eta,\zeta,t) = \hat{\mathbf{q}}(\xi,\eta)\exp\left[\mathrm{i}\left(\int_{\xi_0}^{\xi}\alpha(\xi')\,\mathrm{d}\xi' + \beta\zeta - \omega t\right)\right], \tag{7}$$

where the unknown, streamwise varying wavenumber $\alpha(\xi)$ is determined in the course of the solution by imposing an additional constraint

$$\int_{\eta}\hat{\mathbf{q}}^{H}\frac{\partial\hat{\mathbf{q}}}{\partial\xi}\,h_{\xi}\,h_{\zeta}\,\mathrm{d}\eta = 0, \tag{8}$$

which implies a slow variation of the amplitude functions $\hat{\mathbf{q}}(\xi,\eta,\zeta) = (\hat{\rho},\hat{u},\hat{v},\hat{w},\hat{T})^T$ in the streamwise direction in comparison with the phase term $\exp\left[\mathrm{i}\int_{\xi_0}^{\xi}\alpha(\xi')\,\mathrm{d}\xi'\right]$. Substituting Eq. (7) into the LNS equations and involving the scale separation to neglect the viscous, streamwise derivative terms, one obtains the PSE in the form

$$\left(\mathbf{L} + \mathbf{M}\frac{\partial}{\partial\xi}\right)\hat{\mathbf{q}}(\xi,\eta) = 0. \tag{9}$$

The entries of the coefficient matrices for **L** and **M** with a more detailed description of the method can be found in Refs. [6, 36, 37].

The nonparallel growth rate of the disturbance with a selected combination of ω and β is defined as

$$\sigma_{PSE}(\xi,\omega,\beta) = -\Im(\alpha) + \frac{1}{2}\frac{dE}{d\xi}, \tag{10}$$

and is based on the Mack's energy norm E calculated with

$$E(\xi) = \int_{\eta}\tilde{\mathbf{q}}(\xi,\eta)^{H}\mathbf{M}_E\tilde{\mathbf{q}}(\xi,\eta)\,h_{\xi}\,h_{\zeta}\,\mathrm{d}\eta, \tag{11}$$

where $\mathbf{M}_E$ is the energy weight matrix,

$$\mathbf{M}_E = \mathrm{diag}\left[\frac{\bar{T}(\xi,\eta)}{\gamma\bar{\rho}(\xi,\eta)M^2}, \bar{\rho}(\xi,\eta), \bar{\rho}(\xi,\eta), \bar{\rho}(\xi,\eta), \frac{\bar{\rho}(\xi,\eta)}{\gamma(\gamma-1)\bar{T}(\xi,\eta)M^2}\right]. \tag{12}$$

III. Results

We begin with a brief overview of the CRM-NLF configuration. Following that, the mean flow solution at the selected flow condition is outlined. Then, preliminary results pertaining to the instability amplification at selected spanwise locations of the wing are described. The final paper will include a detailed analysis of the amplification characteristics based on the LST and the PSE with the latter set of results including the effects of both surface curvature and nonparallel development of the boundary layer flow. The N-factor value at the measured transition locations as a function of the wing span location will be documented for multiple flow conditions.

A. Mean Flow Solutions

The CRM is an open geometry representation of a generic transport vehicle and has been used in a multitude of studies [38]. The CRM-NLF builds upon this geometry by replacing the wing with a new one that supports NLF only on the upper surface of the wing and designed using the CDISC NLF design method [39]. The wind-tunnel model is a 5.2% scaled semispan model of the CRM-NLF. The model has a semispan length of 60.151 in., mean aerodynamic chord of 14.342 in. and a leading-edge sweep of 37.3° outboard of break (reduced to 12.9° over the inboard 10% of the wing). More details on the model geometry can be found in Ref. [40] and the CRM webpage (`https://Commonresearchmodel.larc.nasa.gov/crm-nlf`).

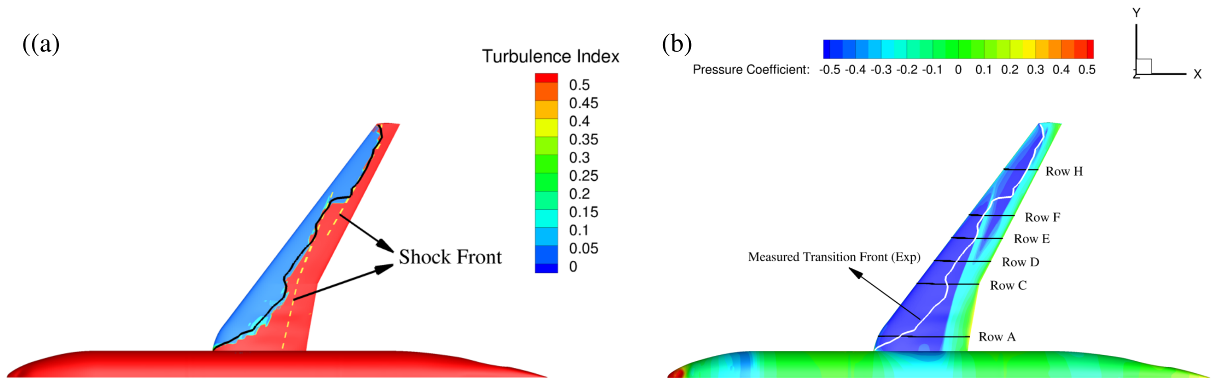

Fig. 1 Surface contours of the (a) turbulent index and (b) pressure coefficient in the imposed transition front solution with SST-2003 RANS model using OVERFLOW of the CRM-NLF configuration at $M_\infty = 0.856$, $AoA = 1.5°$, and $Re_{MAC} = 15 \times 10^6$.

The basic flow has been computed using NASA's OVERFLOW 2.2o [41]. OVERFLOW is an implicit structured overset grid Navier-Stokes solver that is capable of computing time-accurate and steady-state solutions via a variety of options for spatial and temporal discretization. The CRM-NLF computations shown in this abstract are run at conditions of Mach $M_\infty = 0.856$, a Reynolds number-based on the mean aerodynamic chord (MAC) equal to $Re_{MAC} = 15 \times 10^6$ and an angle of attack of $AoA = 1.5°$, that corresponded to one of the experimental test conditions. The free stream turbulence intensity was prescribed to be 0.24%, based on the previous characterization of the tunnel disturbance environment [42]. The conditions corresponding to other freestream conditions and angles of attack will be reported in the final paper. The computations are carried out by using the year 2003 version of Menter's shear-stress transport (SST) RANS model [43] with imposed transition front, so that the flow remained in a laminar state until the specified location of transition, to allow for performing transition stability analysis. The solutions are obtained by running the flow solver in a steady-state manner by using the 3^{rd}-order Roe upwind scheme [44] and the unfactored successive symmetric over relaxation (SSOR) implicit solution algorithm [45]. The computational grid has six overset near-body blocks (three on the fuselage, one wing-body collar grid, and two on the wing, including its tip). The generation of off-body grids and hole-cutting are carried out using OVERFLOW's domain connectivity function (DCF) approach. The grid has a near-wall spacing of $y^+ \approx 0.24$, based on the conditions at 10% of the MAC of the wing, and has approximately 40 wall-normal nodes along the boundary layer thickness and 400 nodes around the wing in the chordwise direction. The turbulent index and the surface pressure coefficient are shown in Fig. 1. Pressure coefficients were measured at selected wing semispan locations that are marked in Fig. 1(b). Figure 2 shows a good agreement of the pressure coefficients between the experiment and the mean flow solution.

B. Instability Characteristics

The stability analysis is performed at selected semispan locations of the CRM-NLF configuration at $M_\infty = 0.856$, $AoA = 1.5°$, and $Re_{MAC} = 15 \times 10^6$. The NASA's LASTRAC solver [36, 37] is used. For three-dimensional boundary layers, a clear distinction between TS and traveling CF waves is often not possible because only a single unstable mode is found. Therefore, a two-dimensional sweep in the disturbance frequency and spanwise wavelength domain must be performed in order to extract the overall N-factor envelope. Figure 3 shows the N-factor curves computed with LST for disturbance frequencies of $f \in [0, 50]$ kHz with $\Delta f = 2$ kHz and spanwise wavelengths of $\lambda \in [0.5, 9]$ mm with $\Delta\lambda = 0.5$ mm. The results for Row C ($\eta_w = 0.370$) of Fig. 3(a) indicate a plateau in the N-factor curves near the measured transition location $\xi_{tr} = 0.1511$ m and the peak N-factor at this location, $N_{tr} = 5.4$, is reached by the disturbance with $f = 8$ kHz and $\lambda = 1$ mm. Results for Row F and Row H of Figs. 3(b) and 3(c), respectively, share a mutually similar trend in the N-factor curves and similar values of the N-factor at the transition location, i.e., $N_{tr} = 7.8$ at $s_{tr} = 0.0789$ m for a disturbance with $f = 18$ kHz and $\lambda = 1$ mm for Row F and $N_{tr} = 7.5$ at $\xi_{tr} = 0.0969$ m for a disturbance with $f = 12$ kHz and $\lambda = 1$ mm for Row H. Thus, there is a large scatter in the LST based N_{tr} values along the wingspan. A more detailed stability analysis based on both LST and PSE, including the effects of nonparallel mean flow, surface curvature, and 3D wave propagation within the boundary layer over the NLF-CRM wing will be presented

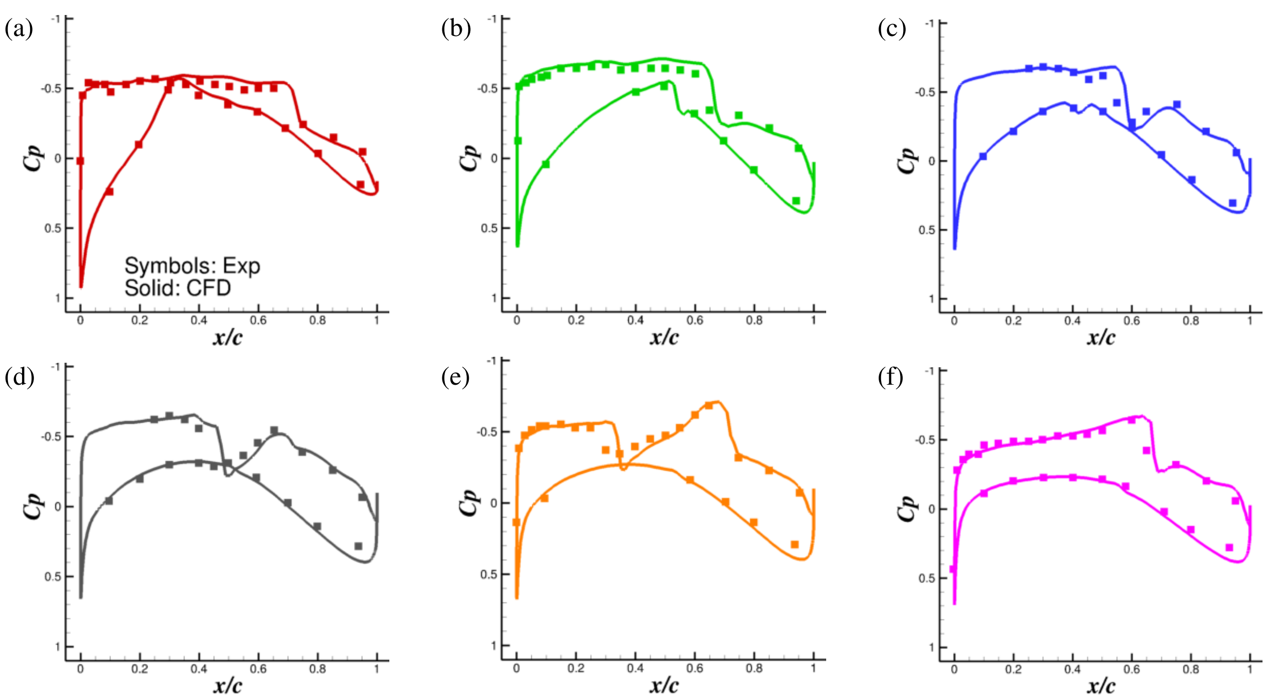

Fig. 2 Numerical (solid lines) and experimental (symbols) pressure coefficients at selected sections of the wing: (a) Row A ($\eta_w = 0.163$), (b) Row C ($\eta_w = 0.370$), (c) Row D ($\eta_w = 0.460$), (d) Row E ($\eta_w = 0.550$), (e) Row F ($\eta_w = 0.640$), and (f) Row H ($\eta_w = 0.820$). The conditions of the selected configuration are $M_\infty = 0.856$, $AoA = 1.5°$, and $Re_{MAC} = 15 \times 10^6$.

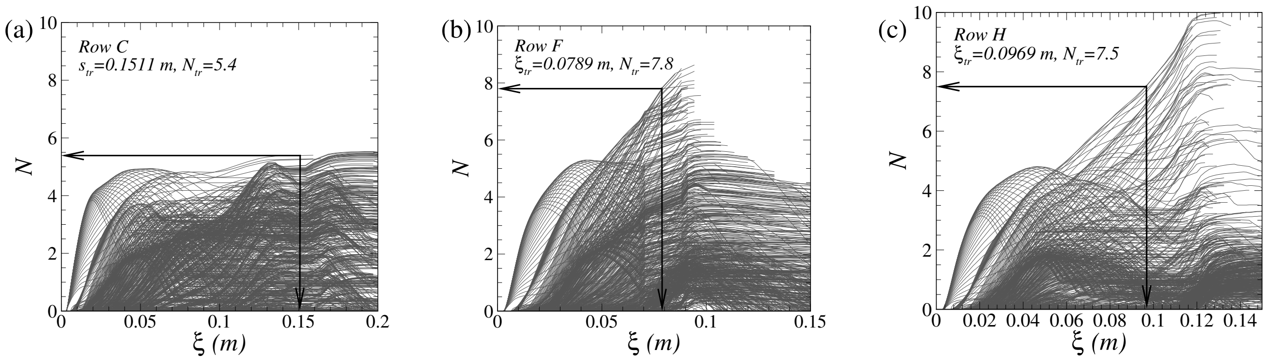

Fig. 3 N-factor calculations based on LST for a range of disturbance frequencies of $f \in [0, 50]$ kHz and spanwise wavelengths of $\lambda \in [0.5, 9]$ mm at selected sections of the wing: (a) Row C ($\eta_w = 0.370$), (b) Row F ($\eta_w = 0.640$), and (c) Row H ($\eta_w = 0.820$). The conditions of the selected configuration are $M_\infty = 0.856$, $AoA = 1.5°$, and $Re_{MAC} = 15 \times 10^6$.

in the final paper for selected experimental conditions.

IV. Summary and Concluding Remarks

Linear stability analysis of the three-dimensional boundary layer flow over the CRM-NLF aircraft configuration is presented. Flow conditions are selected to match those from a recent wind tunnel experiment in the National Transonic Facility at the NASA Langley Research Center [28–30]. The mean flow solution is calculated with the OVERFLOW 2.2o flow solver by specifying the measured laminar-turbulent transition front along the wingspan and by using a Reynolds-Averaged-Navier-Stokes (RANS) turbulence model within the turbulent parts of the flow. The pressure coefficients are found to agree with the measured values at selected wingspan stations. Preliminary results based on the linear stability theory (LST), which assumes the boundary layer profiles to be locally parallel at any given location, show a significant scatter in the logarithmic amplification factor along the measured transition front. Specifically, we find correlating N-factor values of $N_{tr} = 5.4$, 7.8, and 7.5 at spanwise stations C, F, and H, respectively. A comprehensive stability analysis with LST and parabolized stability equations (PSE) that include the effects of surface curvature, nonparallel basic state, and three-dimensional wave propagation will be presented in the final paper for additional freestream conditions and angles of attack.

The CRM-NLF configuration supports the simultaneous presence of multiple transition mechanisms (namely, attachment-line instabilities, Tollmien-Schlichting waves, and stationary and traveling crossflow vortices) at realistic flight transport conditions, which poses a significant challenge even for the state-of-the-art transition models that are nonetheless calibrated with canonical low-speed configurations. The stability results presented herein should provide a useful guidance to improve the physical basis of the existing transition models as described in the accompanying paper by Venkatachari et al. [31].

Acknowledgments

This research is sponsored by the NASA Transformational Tools and Technologies (TTT) Project of the Transformative Aeronautics Concepts Program (TACP) under the Aeronautics Research Mission Directorate (ARMD).

References

[1] *Subsonic Fixed Wing Project Overview*, NASA FAP 2008 Annual Meeting, Atlanta, 2008.

[2] Report of the Group of Personalities, "European Aeronautics: A Vision for 2020," Europan Commission Rept. KI-34-01-827-EN-C, January 2001.

[3] Slotnick, J., Khodadoust, A., Alonso, J., Darmofal, D., Gropp, W., Lurie, E., and Mavriplis, D., "CFD Vision 2030 Study: A Path to Revolutionary Computational Aerosciences," Tech. Rep. CR-2014-218178, NASA, 2014.

[4] Smith, A. M. O., and Gamberoni, N., "Transition, Pressure Gradient and Stability Theory," Tech. Rep. ES-26388, Douglas Aircraft Division, 1956.

[5] Ingen, J. L. v., "A Suggested Semi-Empirical Method for the Calculation of the Boundary Layer Transition Region," *Technische Hogeschool Delft, Vliegtuigbouwkunde, Rapport VTH-74*, 1956.

[6] Herbert, T., "Parabolized Stability Equations," *Annual Review of Fluid Mechanics*, Vol. 29, No. 1, 1997, pp. 245–283. doi:10.1146/annurev.fluid.29.1.245.

[7] Campbell, R., Campbell, M., and Streit, T., "Progress Toward Efficient Laminar Flow Analysis and Design," AIAA Paper 2011-3527, 2011. doi:10.2514/6.2011-3527.

[8] Cliquet, J., Houdeville, R., and Arnal, D., "Application of Laminar-Turbulent Transition Criteria in Navier-Stokes Computations," *AIAA Journal*, Vol. 46, No. 5, 2008, pp. 1182–1190. doi:10.2514/1.30215.

[9] Davis, M. B., Reed, H., Youngren, H., Smith, B., and Bender, E., "Transition Prediction Method Review Summary for the Rapid Assessment Tool for Transition Prediction (RATTraP)," Tech. Rep. AFRL-VA-WP-TR-2005-3130, Lockheed Martin Corporation, June 2005.

[10] Drela, M., "Implicit Implementation of the Full En̂ Transition Criterion," AIAA Paper 2003-4066, Jun 2003. doi:10.2514/6.2003-4066.

[11] Drela, M., and Giles, M. B., "Viscous-Inviscid Analysis of Transonic and Low Reynolds Number Airfoils," *AIAA Journal*, Vol. 25, No. 10, 1987, pp. 1347–1355. doi:10.2514/3.9789.

[12] Krumbein, A., Krimmelbein, N., and Grabe, C., "Streamline-Based Transition Prediction Techniques in an Unstructured Computational Fluid Dynamics Code," *AIAA Journal*, Vol. 55, No. 5, 2017, pp. 1548–1564. doi:10.2514/1.J054990.

[13] Krumbein, A. M., "Automatic Transition Prediction and Application to Three-Dimensional Wing Configurations," *Journal of Aircraft*, Vol. 44, No. 1, 2007, pp. 119–133. doi:10.2514/1.22254.

[14] Perraud, J., Arnal, D., Casalis, G., Archambaud, J.-P., and Donelli, R., "Automatic Transition Predictions using Simplified Methods," *AIAA Journal*, Vol. 47, No. 11, 2009, pp. 2676–2684. doi:10.2514/1.42990.

[15] Stock, H. W., and Haase, W., "Navier-Stokes Airfoil Computations with E Transition Prediction Including Transitional Flow Regions," *AIAA Journal*, Vol. 38, No. 11, 2000, pp. 2059–2066. doi:10.2514/2.893.

[16] Warren, E. S., and Hassan, H. A., "Transition Closure Model for Predicting Transition Onset," *Journal of Aircraft*, Vol. 35, No. 5, 1998, pp. 769–775. doi:10.2514/2.2368.

[17] Edwards, J. R., Roy, C. J., Blottner, F. G., and Hassan, H. A., "Development of a One-Equation Transition/Turbulence Model," *AIAA Journal*, Vol. 39, No. 9, 2001, pp. 1691–1698. doi:10.2514/2.1526.

[18] Walters, D. K., and Leylek, J. H., "A New Model for Boundary Layer Transition using a Single-Point RANS Approach," *Journal of Turbomachinery*, Vol. 126, No. 1, 2004, pp. 193–202.

[19] Menter, F. R., Langtry, R., and Völker, S., "Transition Modelling for General Purpose CFD Codes," *Flow, Turbulence and Combustion*, Vol. 77, No. 1, 2006, pp. 277–303. doi:10.1007/s10494-006-9047-1.

[20] Langtry, R. B., and Menter, F. R., "Correlation-Based Transition Modeling for Unstructured Parallelized Computational Fluid Dynamics Codes," *AIAA Journal*, Vol. 47, No. 12, 2009, pp. 2894–2906. doi:10.2514/1.42362.

[21] Medida, S., and Baeder, J., "Application of the Correlation-Based $\gamma - Re_{\theta}t$ Transition Model to the Spalart-Allmaras Turbulence Model," AIAA Paper 2011-3979, 2011. doi:10.2514/6.2011-3979.

[22] Wang, S., Liang with Fu, "RANS Modeling of High-Speed Aerodynamic Flow Transition with Consideration of Stability Theory," *Progress in Aerospace Sciences*, Vol. 58, 2013, pp. 36–59. doi:10.1016/j.paerosci.2012.08.004.

[23] Ge, X., Arolla, S., and Durbin, P., "A Bypass Transition Model Based on the Intermittency Function," *Flow, Turbulence and Combustion*, Vol. 93, No. 1, 2014, pp. 37–61.

[24] Coder, J. G., and Maughmer, M. D., "Computational Fluid Dynamics Compatible Transition Modeling using an Amplification Factor Transport Equation," *AIAA Journal*, Vol. 52, No. 11, 2014, pp. 2506–2512. doi:10.2514/1.J052905.

[25] Coder, J. G., "Further Development of the Amplification Factor Transport Transition Model for Aerodynamic Flows," AIAA Paper 2019-0039, Jan 2019. doi:10.2514/6.2019-0039.

[26] Medida, S., "Correlation-Based Transition Modeling for External Aerodynamic Flows," Ph.D. thesis, University of Maryland, 2014.

[27] Krumbein, A., Krimmelbein, N., Grabe, C., and Shengyang, N., "Development and Application of Transition Prediction Techniques in an Unstructured CFD Code (Invited)," AIAA Paper 2015-2476, 2015. doi:10.2514/6.2015-2476.

[28] Lynde, M. N., Campbell, R. L., Rivers, M. B., Viken, S. A., Chan, D. T., Watkins, A. N., and Goodliff, S. L., "Preliminary Results from an Experimental Assessment of a Natural Laminar Flow Design Method," AIAA Paper 2019-2298, 2019. doi:10.2514/6.2019-2298.

[29] Lynde, M. N., Campbell, R. L., and Viken, S. A., "Additional Findings from the Common Research Model Natural Laminar Flow Wind Tunnel Test," AIAA Paper 2019-3292, 2019. doi:10.2514/6.2019-3292.

[30] Rivers, M. B., Lynde, M. N., Campbell, R. L., Viken, S. A., Chan, D. T., Watkins, A. N., and Goodliff, S. L., "Experimental Investigation of the NASA Common Research Model with a Natural Laminar Flow Wing in the NASA Langley National Transonic Facility," AIAA Paper 2019–2189, 2019. doi:10.2514/6.2019-2189.

[31] Venkatachari, B., Paredes, P., Derlaga, J., Buning, P., Chouhdari, M., Li, F., and Chang, C.-L., "Assessment and Improvement of RANS-Based Transition Models Based on Experimental Data of the Common Research Model with Natural Laminar Flow," submitted to the AIAA Aviation 2020 Forum, 2020.

[32] Bridges, T. J., and Morris, P. J., "Differential Eigenvalue Problems in Which the Parameter Appears Nonlinearly," *Journal of Computational Physics*, Vol. 55, No. 3, 1984, pp. 437–460.

[33] Malik, M. R., "Numerical Methods for Hypersonic Boundary Layer Stability," *Journal of Computational Physics*, Vol. 86, 1991, pp. 376–413.

[34] Paredes, P., "Advances in Global Instability Computations: from Incompressible to Hypersonic Flow," Ph.D. thesis, Universidad Politécnica de Madrid, 2014.

[35] Canuto, C., Hussaini, M. Y., Quarteroni, A., and Zang, T. A., *Spectral methods in fluid dynamics*, Springer, 1987.

[36] Chang, C.-L., "LASTRAC.3d: Transition Prediction in 3D Boundary Layers," AIAA Paper 2004-2542, 2004.

[37] Chang, C.-L., "Langley Stability and Transition Analysis Code (LASTRAC) Version 1.2 User Manual," NASA TM-2004-213233, 2004.

[38] Vassberg, J. C., DeHaan, M. A., Rivers, M. S., and Wahls, R. A., "Restrospective on the Common Research Model for Computational Fluid Dynamics Validation Studies," *Journal of Aircraft*, Vol. 55, No. 4, 2018, pp. 1325–1337. doi: 10.2514/1.C034906.

[39] Campbell, R. L., and Lynde, M., "Expanding the Natural Laminar Flow Boundary for Supersonic Transports," AIAA Paper 2016-4327, 2016. doi:10.2514/6.2016-4327.

[40] Lynde, M. N., and Campbell, R. L., "Computational Design and Analysis of a Transonic Natural Laminar Flow Wing for a Wind Tunnel Model," AIAA Paper 2017-3058, 2017. doi:10.2514/6.2017-3058.

[41] Nichols, H., and Buning, P., "User's Manual for OVERFLOW 2.2," , August 2000. URL `https://overflow.larc.nasa.gov/home/users-manual-for-overflow-2-2/`.

[42] Crouch, J., Sutanto, M., Witkowski, D., Watkins, A., Rivers, M., and Campbell, R., "Assessment of the National Transition Facility for Natural Laminar Flow Testing," AIAA Paper 2010-1302, 2010. doi:10.2514/6.2010-1302.

[43] Menter, F. R., Kuntz, M., and Langtry, R., "Ten Years of Industrial Experience with the SST Turbulence Model," *Turbulence, heat and mass transfer*, Vol. 4, No. 1, 2003, pp. 625–632.

[44] Roe, P. L., "Approximate Riemann Solvers, Parameter Vectors, and Difference Schemes," *Journal of computational physics*, Vol. 43, No. 2, 1981, pp. 357–372.

[45] Nichols, R., Tramel, R., and Buning, P., "Solver and Turbulence Model Upgrades to OVERFLOW 2 for Unsteady and High-Speed Applications," AIAA Paper 2006-2824, 2006. doi:10.2514/6.2006-2824.